SPANDIDOS
PUBLICATIONS

Systematic pan-cancer analysis identifies CDC45 as having an oncogenic role in human cancers

YALIN LU[1-3*], XINGJIE CHEN[1-3*], FANG LIU[4*], HAO YU[1-3], YU ZHANG[1-3],
KANGJIE DU[1-3], YANG NAN[1-3,5] and QIANG HUANG[1-3,5]

[1]Department of Neurosurgery, Tianjin Medical University General Hospital; [2]Key Laboratory of Post-Trauma
Neuro-Repair and Regeneration in Central Nervous System, Ministry of Education; [3]Tianjin Key Laboratory of
Injuries, Variations and Regeneration of Nervous System, Tianjin Medical University General Hospital; [4]Institute of
Mental Health, Tianjin Anding Hospital, Mental Health Center of Tianjin Medical University, Tianjin 300052;
[5]Department of Neurosurgery, Tianjin Medical University General Hospital Airport Site, Tianjin 300308, P.R. China

Abstract. Cell division cycle 45 (CDC45) is an essential protein required for the initiation of DNA replication. In the present study, the role of CDC45 across 33 cancers was systematically investigated. It was observed that the expression of CDC45 was significantly upregulated in most cancers, exhibiting a marked negative correlation with the overall survival. Next, there was no significant difference in prognosis between the genomically altered and unaltered groups with respect to clinical outcomes. A decreased level of CDC45 at the DNA promoter region was also identified in several cancers. Furthermore, CDC45 expression was associated with the levels of tumor-infiltrating immune cells in some specific cancer types. In addition, CDC45 was associated with m6A methylation, and CDC45 expression was primarily positively correlated with 'writers' and 'readers' in various cancers, particularly HNRNPC, RBM15 and YTHDC1. Gene enrichment analysis was also performed. In addition, the AUC of each cancer with respect to its 1-, 3-, and 5-year survival rates were explored. Finally, CCK-8 assays, EdU assays and cell cycle analysis were conducted. In conclusion, the present study demonstrated that CDC45 may be a potential biomarker and target for cancer treatment.

Correspondence to: Professor Qiang Huang, Department of Neurosurgery, Tianjin Medical University General Hospital, 154 Anshan Road, Heping District, Tianjin 300052, P.R. China
E-mail: huangqiang209@163.com

*Contributed equally

Introduction

With the development of science and technology, much progress has been made over the past decade in the development of novel treatments, including surgery, radiation, chemotherapy, immunotherapy, hormone therapy, and targeted therapy, but the overall therapeutic effects are still not satisfactory (1-3). Thus, clarifying the mechanisms of cancer pathogenesis and tumorigenesis remain important for identifying novel tumor treatments.

Cell division cycle 45 (CDC45), which contains 21 exons located at 22q11.21, is a critical component of the eukaryotic DNA replisome. CDC45 plays an essential role in the replicative helicase holoenzyme CDC45-MCM-GINS complex, activating MCM2-7 and resulting in DNA replication and unwinding (4-7). Knocking down CDC45 suppresses DNA replication and inhibits cell proliferation in human cells (8). A previous study demonstrated that the protein levels of CDC45 are highly expressed in human cancer-derived cells compared to primary cells (9). In addition, high expression of CDC45 recapitulates all c-Myc-induced replication and damage phenotypes, and CDC45 and GINS both function downstream of Myc (10).

Recently, several bioinformatics studies have demonstrated the role of CDC45 in different cancers, such as colorectal cancer (11), non-small cell lung cancer (12,13), esophageal squamous cell carcinoma (14), and hepatocellular carcinoma (15-17), but only one experimental study has examined the roles of CDC45 in tumorigenesis (18). Currently, there is no pan-cancer analysis of the function of CDC45 across different cancers.

In the present study, multiple databases were searched, including The Cancer Genome Atlas (TCGA), Genotype-Tissue Expression (GTEx), ONCOMINE, Tumor Immune Estimation Resource (TIMER), tumor-immune system interactions database (TISIDB), Human Protein Atlas (HPA), MEXPRESS, Gene Expression Profiling Interactive Analysis (GEPIA), UALCAN, cBioPortal, RNA Epitranscriptome Collection (REPIC), N6-methyladenosine (m6A)-Atlas and Search Tool

for the Retrieval of Interacting Genes/Proteins (STRING), to explore the function of CDC45 across 33 types of cancer. The RNA and protein expression levels of CDC45 were first analyzed in different cancers, followed by the examination of the association between CDC45 expression and overall survival (OS) and disease-free survival (DFS). Second, the genetic mutations of CDC45 were explored. The association between CDC45 and immunity, including tumor mutation burden (TMB), microsatellite instability (MSI), and immune subtype were also explored. Subsequently, DNA methylation, m^{6}A and receiver operating characteristic curve (ROC) were examined across 33 cancers. In addition, co-expressed proteins were searched for and Gene Ontology (GO) and Kyoto Encyclopedia of Genes and Genomes (KEGG) analyses were performed. Finally, Cell Counting Kit-8 (CCK-8) assays, 5-ethynyl-2'-deoxyuridine (EdU) proliferation assays and cell cycle analysis were performed to validate the roles of CDC45 *in vitro*. The present results indicated that CDC45 plays an important role in tumorigenesis across 33 different cancer types, which may represent a new strategy for tumor prognosis and treatment.

Materials and methods

TCGA. TCGA is a comprehensive, freely accessible database that contains over 20,000 primary cancer and matched normal samples across 33 cancer types (https://www.cancer.gov/about-nci/organization/ccg/research/structural-genomics/tcga). It provides high dimensionality and quality data, including genomic, epigenomic, transcriptomic, and proteomic data. The details of the data include clinical, gene expression, copy number variation, mutation, methylation and protein (19).

Genotype-tissue expression (GTEx). GTEx (https://www.gtexportal.org/) contains genotype data of nearly 17,382 RNA-seq samples across 54 tissue sites (from 948 postmortem donors) and 2 cell lines. Full gene expression datasets are available for free. This portal established a comprehensive catalog of genetic variants that affect gene expression across multiple tissues, for the research community, to evaluate tissue-specific gene expression and regulation in numerous different tissues.

Oncomine database. Oncomine (https://www.oncomine.org) is a public database that can easily obtain microarray data across different cancers. The mRNA levels of CDC45 were compared between cancer and control tissues using the following threshold: P<0.05; fold change, >2; gene rank, Top 10%.

TISIDB database. TISIDB (http://cis.hku.hk/TISIDB/index.php) is an online website that focuses on the interactions between cancer and the immune system and contains multiple heterogeneous data types (20). The association between CDC45 expression and the grade or stage of different cancers from TCGA was investigated. In addition, it was also used to analyze the interaction between CDC45 levels in different immune subtypes, including C1 (wound healing), C2 (IFN-γ dominant), C3 (inflammatory), C4 (lymphocyte depleted), C5 (immunologically quiet), and C6 (TGF-β dominant).

TIMER. TIMER (http://timer.cistrome.org/) is a comprehensive online website to explore tumor immunological, clinical and genomic features (21). Moreover, gene correlation analysis was also performed using TIMER across 32 cancers. The 'Expression' module was searched using the keyword 'CDC45' for CDC45 expression in different cancers and matched normal samples from TCGA. Similarly, the 'Immune' module was used to investigate the correlation between CDC45 and different immune cells, including CD8$^+$ T cells, CD4$^+$ T cells, neutrophils, myeloid dendritic cells, macrophages, and B cells, across all TCGA cancers. Moreover, the 'Gene_Corr' module was adopted to determine the correlation between CDC45 and m^{6}A-related genes.

HPA. HPA (https://www.proteinatlas.org/) has collected the entire human proteome and characterized it using immunohistochemistry and immunocytochemistry (22). It is also used to detect protein localization and expression in human tissues and cells. From this program, immunohistochemical images of different cancers and matched normal samples were downloaded.

cBioPortal. The cBioPortal (https://www.cbioportal.org/) is an open source that contains gene data, including mutation and putative copy number alterations (CNVs) (23). The 'TCGA Pan Cancer Atlas Studies' in 'Quick select' was searched using the keyword 'CDC45' for gene mutations and CNVs across 32 cancers. Then, the summary results in the 'Cancer Types Summary' module were obtained. In addition, the details of mutated information of CDC45 are displayed in the diagram of protein structure or 3D graphics. Furthermore, the correlation between CDC45 mutation and clinical outcomes was explored using the 'Comparison/Survival' module.

GEPIA. GEPIA is an interactive website for exploring RNA-seq expression from TCGA and GTEx based on the normalized processing pipeline (http://gepia2.cancer-pku.cn/#index). It provides differential expression analysis, cancer type, pathological grade, survival analysis, similar gene detection and correlation analysis (24). By searching different modules, the correlation between CDC45 expression and cancer stage, OS and DFS across 33 cancers was analyzed using the following CDC45 cutoff value: High, 50%; low, 50%. Similar genes for GO and KEGG analyses were also downloaded.

UALCAN. The UALCAN (http://ualcan.path.uab.edu/index.html) database was used to analyze the DNA methylation of CDC45 between different cancer and matched normal samples from TCGA (25). Herein, we compared the methylation level of the CDC45 promoter region between cancer and matched control tissues and found that five cancer types exhibited significant differences, including bladder urothelial carcinoma (BLCA), breast invasive carcinoma (BRCA), testicular germ cell tumors (TGCTs), lung adenocarcinoma (LUAD) and head and neck squamous cell carcinoma (HNSC).

MEXPRESS. MEXPRESS (https://mexpress.be) is an online website that allows researchers to explore DNA methylation from TCGA (26). Herein, we searched the DNA methylation of BLCA, BRCA, TGCT, LUAD and HNSC to verify the

results obtained from UALCAN, and promoter region probes were obtained.

m⁶A-Atlas. m⁶A-Atlas (http://180.208.58.66/m6A-Atlas/index. html) is a comprehensive online tool for revealing the m⁶A epitranscriptome (27). By selecting 'Human gene' and 'CDC45', detailed results, including m⁶A records, overall distribution pattern of m⁶A sites, and the distribution of all m⁶A sites and RNA binding proteins (RBPs) were obtained.

REPIC. The REPIC (https://repicmod.uchicago.edu/repic) database is an online source that records numerous data retrieved from the Gene Expression Omnibus (GEO) and the Sequence Read Archive (SRA) of m⁶A-seq and MeRIP-seq using their unified pipeline (28). This database is used to query m⁶A modification sites by specific cell lines or tissue types. The m⁶A modification sites in different cell lines or tissues of CDC45 were explored.

STRING. The STRING database (http://string-db.org) is an online server that focuses on protein-protein interactions (PPIs) and functional protein networks (29). By querying 'CDC45' in this database and setting up parameters as follows: Minimum required interaction score ['low confidence (0.150)'], meaning of network edges ('evidence'), max number of interactors to show ('no more than 50 interactors' in 1st shell) and active interaction sources ('experiments, database, co-expression'), the top 50 proteins that bind with CDC45 were obtained.

BioGRID, HIPPIE and HitPredict. BioGRID (https://thebiogrid.org/), HIPPIE (http://cbdm-01.zdv. uni-mainz.de/~mschaefer/hippie/) and HitPredict (http://www. hitpredict.org/) databases were searched for PPI analysis.

LinkedOmics. LinkedOmics (http://linkedomics.org/login. php) is a publicly available portal that provides a unique platform for biologists and clinicians to access, analyze and compare cancer multi-omics data within and across tumor types.

R software. To analyze TCGA and GTEx data, R (version 3.6.3) software (https://cran.r-project. org/bin/windows/base/old/3.6.3/) was used. With regard to certain cancers without control samples or those with highly limited normal tissues, the corresponding samples from GTEx were extracted as control groups, and the 'ggplot2 package' was used to visualize gene expression. The 'ggradar' and 'ggplot2' packages were used to reveal the MSI and neoantigens of immunity. The 'timeROC' package was used to compare the predictive accuracy of CDC45 and the risk score, and the log-rank test was also used to compare the survival difference between the two groups. The 'clusterProfiller' and 'org.Hs.eg.db' packages were used for GO and KEGG analyses. P<0.05 was considered to indicate a statistically significant difference.

Cell culture. Two human GBM cell lines, U251 and glioblastoma of unknown origin U87, were purchased from American Type Culture Collection. Cells were cultured in high-glucose Dulbecco's modified Eagle's medium (DMEM; Corning, Inc.)

supplemented with 10% fetal bovine serum (FBS; Thermo Fisher Scientific, Inc.) at 37°C and 5% CO_2. These cell lines underwent *Mycoplasma* tests and were authenticated by Short Tandem Repeat (STR) analysis (Beijing Microread Genetics Co., Ltd.).

Small interfering RNA (siRNA) sequences. The sequences of CDC45 siRNA (Hanbio Biotechnology Co., Ltd.) were as follows: Negative control (NC), 5'-UUCUCCGAACGUGUC ACGU-3' (sense) and 5'-ACGUGACACGUUCGGAGAA-3' (antisense); siCDC45-1, 5'-GCGUGCAGACUUUCAGCA UTT-3' (sense) and 5'-AUGCUGAAAGUCUGCACGCTT-3' (antisense); and siCDC45-2, 5'-GCAAGACAAGAUCACUCA A-3' (sense)and 5'-UUGAGUGAUCUUGUCUUGC-3' (antisense).

Cell transfection. U87 and U251 cells were seeded into 24- and 96-well plates and transfected 48 h later using Lipofectamine 3000 (Life Technologies Corporation; Thermo Fisher Scientific, Inc.) according to the manufacturer's protocol. Briefly, for 24-well plates, 1 µl siRNA (20 µM) was transfected into target cells using 1.5 µl Lipofectamine 3000 at room temperature. For 96-well plates, 0.2 µl siRNA (20 µM) was transfected into target cells using 0.3 µl Lipofectamine 3000 at room temperature. Following 48 h of incubation at 37°C and 5% CO_2, subsequent experiments were conducted.

RNA extraction and reverse transcription-quantitative PCR (RT-qPCR). Total RNA was extracted from the cells using TRIzol (Takara Biotechnology Co., Ltd.) according to the manufacturer's protocol. cDNA was synthesized using the GoScript Reverse Transcription System (Promega Corporation) and 1 µg of RNA according to the manufacturer's protocol. qPCR was performed using a SYBR Green PCR kit (Bimake. com) according to the manufacturer's instructions on an Applied Biosystems QuantStudio instrument (Thermo Fisher Scientific, Inc.). Comparative quantification was performed using the $2^{-\Delta\Delta Cq}$ (30) method with GAPDH as the endogenous control, The PCR system was 20 µl, and the thermocycling conditions were as follows: 40 cycles were operated at 95°C for 3 min, 95°C for 15 sec and 60°C for 1 min. The dissolution curve program was as follows: 95°C for 15 sec, 60°C for 1 min, and 95°C for 1 sec. The primer sequences were as follows: CDC45 forward, 5'-TTCGTGTCCGATTTCCGCAAA-3' and reverse, 5'-TGGAACCAGCGTATATTGCAC-3'; GAPDH forward, 5'-GGAGCGAGATCCCTCCAAAAT-3' and reverse, 5'-GGCTGTTGTCATACTTCTCATGG-3'.

CCK-8 assay. Following transfection, U87 and U251 cells were divided into 96-well plates at 3x10³ cells per well. At 24, 48, 72, 96, 120, and 144 h, CCK-8 solution was added (10 µl; Beyotime Institute of Biotechnology), and the cells were then incubated for 2 h at 37°C and 5% CO_2. The optical density (OD) at 450 nm (OD_{450}) was then assessed using a microplate reader (Biotek Instruments, Inc.).

Cell-Light EdU proliferation assay. U87 and U251 cells (5x10³/well) were inoculated into 24-well plates. Following 48 h of incubation at 37°C and 5% CO_2, an EdU *In Vitro* Kit (cat. no. C10310-1; Guangzhou RiboBio Co., Ltd.) was

employed based on the manufacturer's protocol. Briefly, the EdU medium mixture (50 μM) was discarded, and 4% paraformaldehyde was added to fix cells at room temperature for 30 min. The cells were then washed with glycine (2 mg/ml) for 5 min on a shaker, and 0.2% Triton X-100 was added for 10 min. The cells were then washed twice with PBS, and click reaction buffer (Tris-HCl, pH 8.5, 100 mM; CuSO4, 1 mM; Apollo 550 fluorescent azide, 100 μM; and ascorbic acid, 100 mM) was added for 10-30 min while protecting from light. Subsequently, the cells were washed three times with 0.5% Triton X-100, and stained with Hoechst (5 μg/ml) for 30 min at room temperature. Finally, the cells were washed five times with 0.5% Triton X-100, and then 150 μl PBS was added. Images were obtained using a fluorescence microscope (magnification, x4; cat. no. IX81; Olympus Corporation).

Cell cycle analysis. The cell cycle was measured using flow cytometry and a detection reagent kit (Nanjing KeyGen Biotech Co., Ltd.) according to the manufacturer's protocols. Briefly, $2x10^6$/well cells were seeded into 6-well plates and cultured for 48 h at 37°C and 5% CO_2. Next, cells were collected using trypsin (Beijing Solarbio Science & Technology Co., Ltd.), washed with PBS (centrifuged at 396 x g for 5 min at 4°C) three times, and fixed in 70% ice-cold ethanol at 4°C overnight. After washing with ice-cold PBS (centrifuged at 742 x g for 5 min at 4°C) twice, cells were stained with 500 μl propidium iodide containing RNase A buffer for 30 min at room temperature away from light. The percentage of cells was calculated and analyzed using a BD FACSAria flow cytometer (BD Biosciences), and the results were interpreted using FlowJo version 10 (BD Biosciences).

Statistical analysis. The experiments were repeated three times independently. Results were analyzed using GraphPad software 8.0 (GraphPad Software, Inc.), and all quantitative data are presented as the means ± SDs. Unpaired Student's t-test was performed to compare differences between two different groups with parametric variables, while one-way ANOVA was used to analyze the significance of multiple group comparisons. Tukey's post hoc test was performed following ANOVA. Spearman's rank correlation coefficient was performed to analyze the strength and direction of association between two ranked variables. The Pearson correlation coefficient was used to assess a linear correlation. All statistical analyses were two-sided, and $P<0.05$ was considered to indicate a statistically significant difference. Variance was similar between the groups being statistically compared.

Results

CDC45 expression in pan-cancer. To analyze CDC45 expression in different cancers, the Oncomine database, was first searched. Compared with noncancerous samples, levels of CDC45 were markedly elevated in various cancers (Fig. 1A). Next, the relative CDC45 expression across different cancers of TCGA were explored using TIMER 2.0. CDC45 expression was higher in BLCA, BRCA, cervical squamous cell carcinoma and endocervical adenocarcinoma (CESC), cholangiocarcinoma (CHOL), colon adenocarcinoma (COAD), esophageal carcinoma

(ESCA), glioblastoma multiforme (GBM), HNSC, kidney chromophobe (KICH), kidney renal clear cell carcinoma (KIRC), kidney renal papillary cell carcinoma (KIRP), liver hepatocellular carcinoma (LIHC), LUAD, lung squamous cell carcinoma (LUSC), pancreatic adenocarcinoma (PAAD), pheochromocytoma and paraganglioma (PCPG), prostate adenocarcinoma (PRAD), rectum adenocarcinoma (READ), stomach adenocarcinoma (STAD), thyroid carcinoma (THCA) and uterine corpus endometrial carcinoma (UCEC) (Fig. 1B) than in matched control samples. With regard to certain cancers without control samples or those with highly limited normal tissues, including adrenocortical carcinoma (ACC), lymphoid neoplasm diffuse large B-cell lymphoma (DLBC), acute myeloid leukemia (LAML), brain lower grade glioma (LGG), ovarian serous cystadenocarcinoma (OV), sarcoma (SARC), skin cutaneous melanoma (SKCM), TGCT, thymoma (THYM), and uterine carcinosarcoma (UCS), GTEx data were utilized as control groups, allowing the further investigation of CDC45 expression between various cancers and their matched control groups. The results revealed that CDC45 was significantly increased in almost all cancers, except for LAML, SARC, mesothelioma (MESO) and uveal melanoma (UVM) (Fig. 1C). The association between CDC45 expression and different cancer stages was further explored in each cancer, and it was determined that CDC45 expression was positively associated with ACC, KICH, KIRC, KIRP, LIHC, LUAD and UCEC, while COAD, OV and READ exhibited negative associations (Fig. 1D). In addition, association between CDC45 expression and different pathological grades of each cancer was evaluated, and the results demonstrated that levels of CDC45 were positively associated with CESC, HNSC, KIRC, LGG, LIHC PAAD and UCEC (Fig. 1E).

As proteins are the substances that execute biological processes, the protein levels of CDC45 across different cancers were next analyzed. Based on HPA, it was revealed that CDC45 protein levels were increased in most cancer tissues compared with matched control samples (Fig. S1).

Prognostic value of CDC45 in various cancers. Given that CDC45 is highly expressed in various cancers, the survival association between CDC45 and different cancers was next analyzed using the TCGA project. The results indicated that high levels of CDC45 were negatively associated with the overall survival in patients with ACC, KICH, KIRC, KIRP, LAML, LGG, LIHC, LUAD, MESO, PAAD, SARC, SKCM and UVM, while CESC showed a positive correlation with OS (Fig. 2). Finally, to further explore the association between CDC45 expression and the predictive ability of OS in different cancers, the raw counts of RNA-sequencing data and clinical information of different cancers from TCGA were downloaded, and time ROC analysis was also performed to compare the predictive accuracy of each gene and the risk score. The area under the ROC curve (AUC) of each cancer in the 1-, 3-, and 5-year survival rates conveyed a high predictive value, especially in ACC (1-year 0.834, 3-year 0.954, and 5-year 0.847), MESO (1-year 0.800, 3-year 0.805, and 5-year 0.856), KICH (1-year 0.983, 3-year 0.758, and 5-year 0.844) and KIRP (1-year 0.739, 3-year 0.769, and 5-year 0.661). These results indicated that CDC45 expression may be a biomarker for the prognosis of these cancers (Fig. 3).
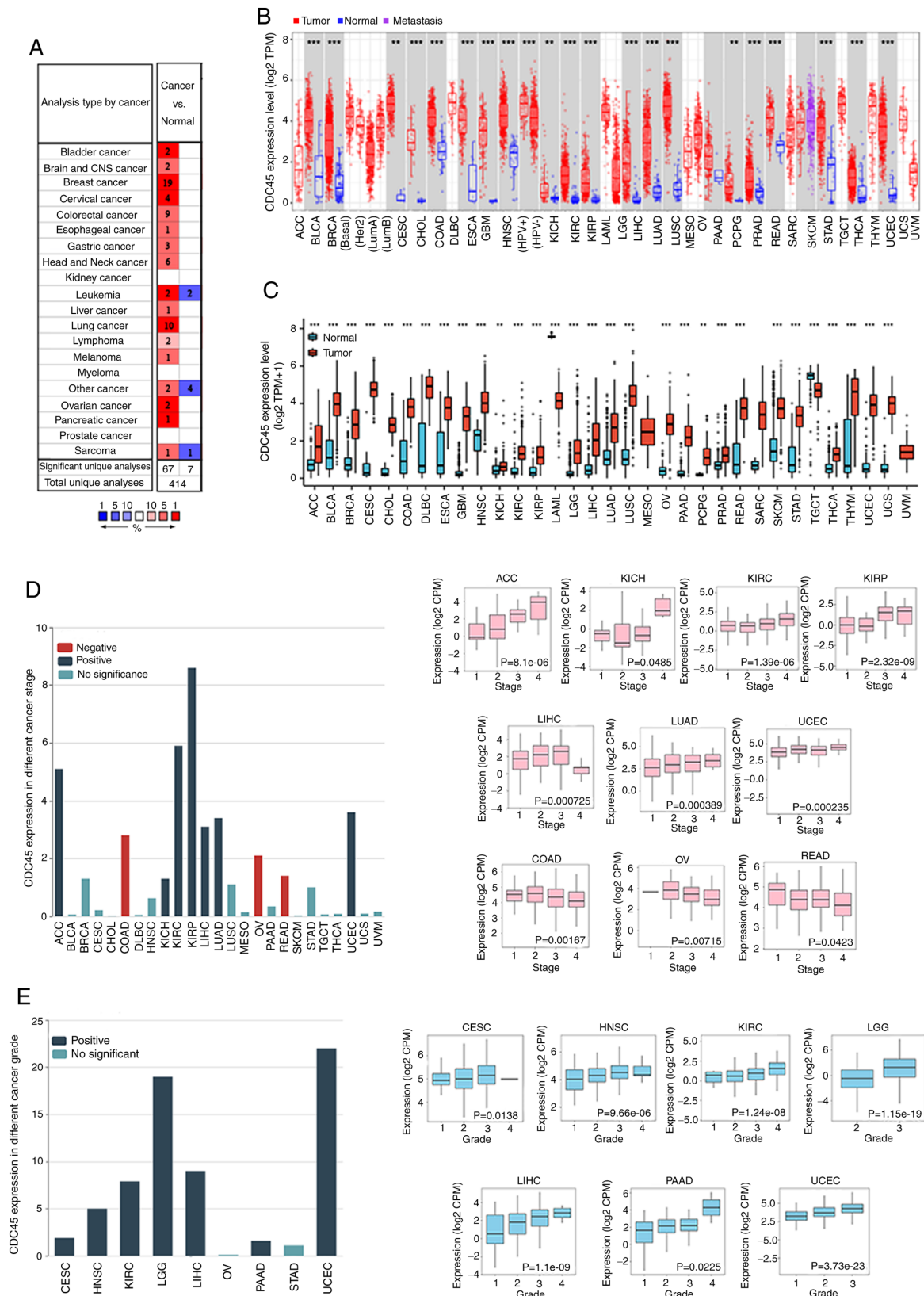
Figure 1. Levels of CDC45 expression in different cancers. (A) CDC45 expression in various cancers compared with control tissues in the Oncomine database. (B) CDC45 expression in different cancers compared with adjacent control tissues from TCGA by TIMER 2.0. (C) CDC45 expression in different cancers between tumors (TCGA) and corresponding control tissues (GTEx). (D) The association between CDC45 expression and different cancer stages in ACC, KICH, KIRC, KIRP, LIHC, LUAD, UCEC, COAD, OV and READ. Red bar, negative association; blue bar, positive association; and cyan bar, no significance. (E) CDC45 expression of different pathological stages in CESC, HNSC, KIRC, LGG, LIHC, PAAD and UCEC. Blue bar, positive association; cyan bar, no significance. **P<0.01 and ***P<0.001. CDC45, cell division cycle 45; TCGA, The Cancer Genome Atlas; TIMER, Tumor Immune Estimation Resource; GTEx, Genotype-Tissue Expression; ACC, adrenocortical carcinoma; KICH, kidney chromophobe; KIRP, kidney renal papillary cell carcinoma; LIHC, liver hepatocellular carcinoma; LUAD, lung adenocarcinoma; UCEC, uterine corpus endometrial carcinoma; COAD, colon adenocarcinoma; OV, ovarian serous cystadenocarcinoma; READ, rectum adenocarcinoma; CESC, cervical squamous cell carcinoma and endocervical adenocarcinoma; HNSC, head and neck squamous cell carcinoma; LGG, brain lower grade glioma; PAAD, pancreatic adenocarcinoma.
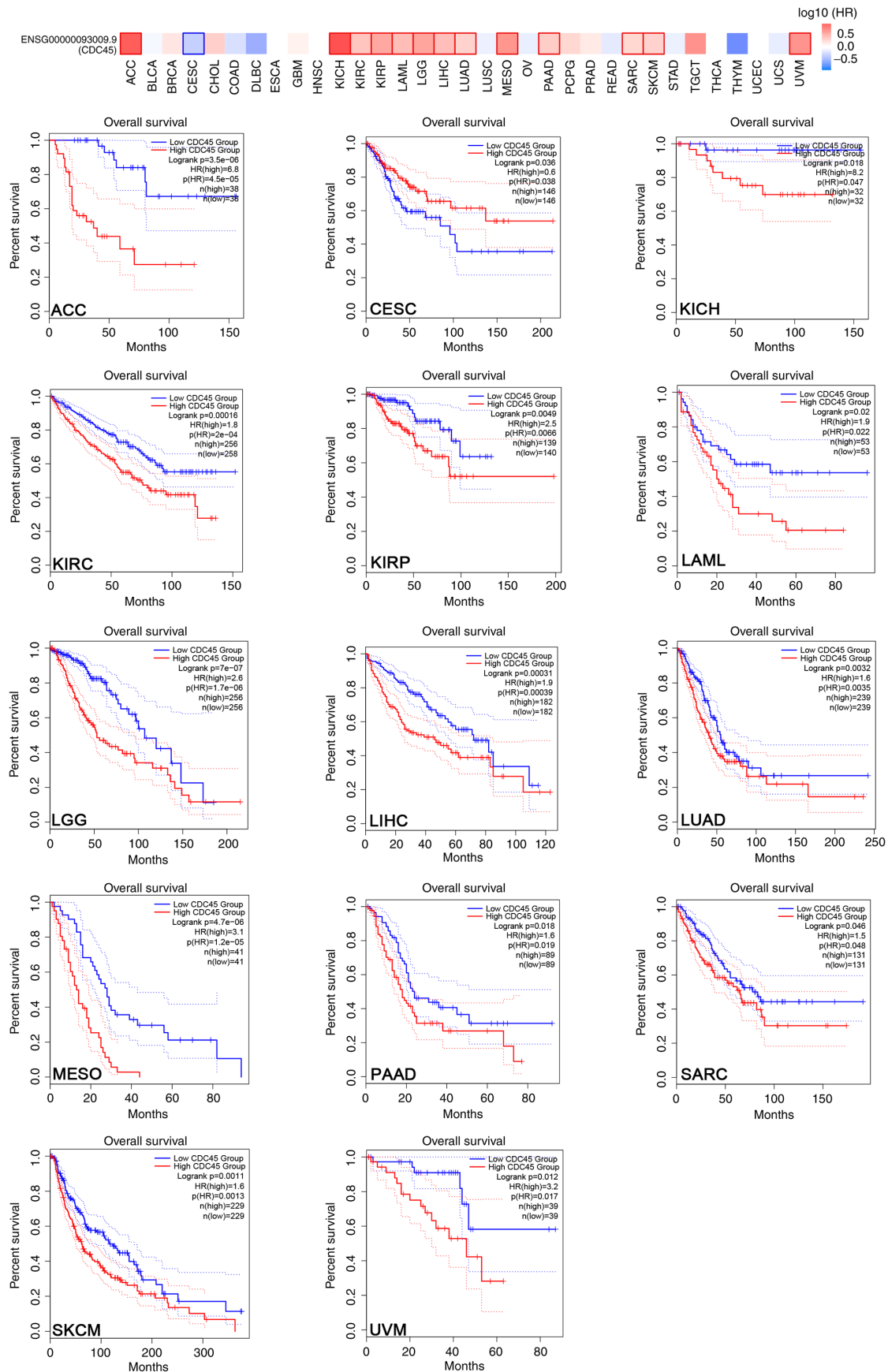
Figure 2. Prognostic value of CDC45 in various cancers. Overall survival analysis of CDC45 expression in different cancers compared with adjacent control tissues from TCGA and GTEx using GEPIA2. CDC45, cell division cycle 45; TCGA, The Cancer Genome Atlas; GTEx, Genotype-Tissue Expression; GEPIA, Gene Expression Profiling Interactive Analysis; ACC, adrenocortical carcinoma; CESC, cervical squamous cell carcinoma and endocervical adenocarcinoma; KICH, kidney chromophobe; KIRC, kidney renal clear cell carcinoma; KIRP, kidney renal papillary cell carcinoma; LAML, acute myeloid leukemia; LGG, brain lower grade glioma; LIHC, liver hepatocellular carcinoma; LUAD, lung adenocarcinoma; MESO, mesothelioma; PAAD, pancreatic adenocarcinoma; SARC, sarcoma; SKCM, skin cutaneous melanoma; UVM, uveal melanoma.
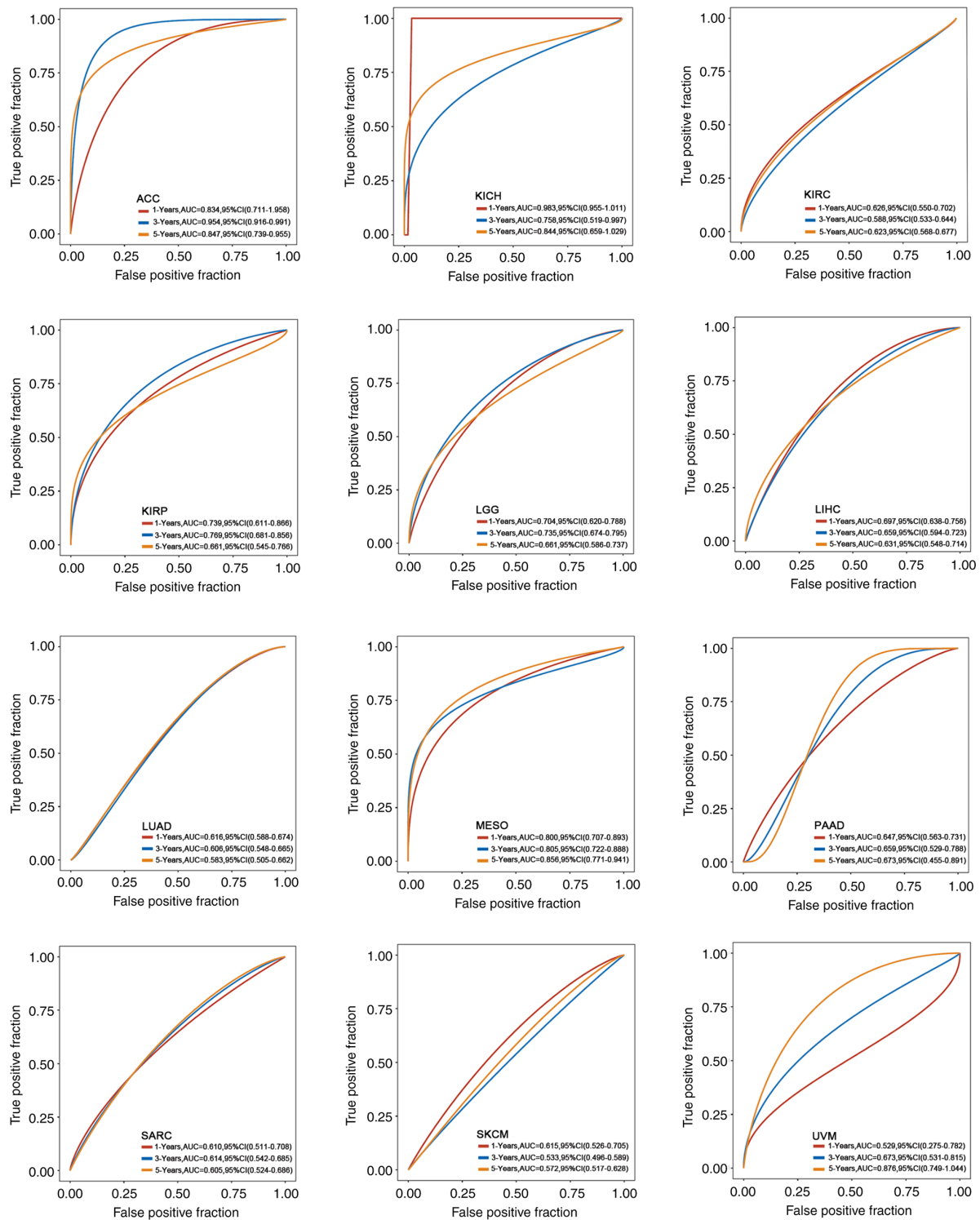
Figure 3. Association between CDC45 expression and the predictive ability of overall survival in different cancers. The raw counts of RNA-sequencing data and clinical information of different cancers from TCGA were downloaded, and timeROC analysis was also performed to compare the predictive accuracy of each gene and the risk score. The AUC of each cancer in the 1-, 3-, and 5-year survival rates are presented. CDC45, cell division cycle 45; TCGA, The Cancer Genome Atlas; ROC, receiver operating characteristic; AUC, area under the ROC curve; ACC, adrenocortical carcinoma; KICH, kidney chromophobe; KIRC, kidney renal clear cell carcinoma; KIRP, kidney renal papillary cell carcinoma; LGG, brain lower grade glioma; LIHC, liver hepatocellular carcinoma; LUAD, lung adenocarcinoma; MESO, mesothelioma; PAAD, pancreatic adenocarcinoma; SARC, sarcoma; SKCM, skin cutaneous melanoma; UVM, uveal melanoma.

CDC45 alteration analysis in various cancers. Next, CDC45 alterations in various cancers from the TCGA database were obtained. As revealed in Fig. S2A, the most frequent genetic alteration was 'mutation' in UCS (7.02%), which was entirely composed of the 'amplification' type, and the same statistical trends occurred in TGCT (1.34%), MESO (1.15%), PCPG (0.56%) and THCA (0.4%). The details of 'mutation' were also explored using a diagram (Fig. S2B), including sites,

types and case numbers. Missense was the most common mutation type of CDC45 mutation (83/101), followed by truncation (10/101), splice (6/101), in frame (1/101) and SV/fusion (1/101). R175 and X163 had 3 mutations, and the mutation type of R175 is presented in the 3D structure of the CDC45 protein (Fig. S2C).*CDC45 and DNA methylation in various cancers.* Subsequently, the DNA promoter methylation levels between different cancers and matched control tissues were investigated using UALCAN. It was observed that the beta values were higher in normal samples than in cancer tissues in BLCA, BRCA, TGCT, LUAD and HNSC (Fig. 4; images on the left). In addition, potential probes of DNA methylation across different cancers were searched using MEXPRESS. As revealed in Fig. 4 (images on the right), all promoter probes were negatively correlated with CDC45 DNA methylation, indicating that DNA promoter methylation is reduced in BLCA, BRCA, TGCT, LUAD and HNSC. These results are consistent with the data obtained from UALCAN, suggesting that the promoter methylation level of CDC45 may participate in the processes of tumorigenesis in BLCA, BRCA, TGCT, LUAD and HNSC.

CDC45 and immunology in various cancers. In recent years, immunotherapy has shown great potential in various cancers. It was next examined whether there were associations between cancers and immunology with respect to CDC45. First, the association between CDC45 and different immune cells, including CD8$^+$ T cells, CD4$^+$ T cells, neutrophils, myeloid dendritic cells, macrophages, and B cells, were analyzed across all TCGA cancers in the TIMER2.0 database. The data revealed that CDC45 was almost positively associated with these immune cells in KIRC, LIHC, THCA and THYM but negatively associated with LUAD, LUSC, and GBM (Fig. 5A). Considering the important role of tumor MSI, which establishes a significant association with the sensitivity to immune checkpoint inhibitors, Fig. 5B revealed that CDC45 was positively associated with MSI in 11 cancers, including HNSC (P=0.017), THCA (P=0.0071), KIRC (P=6.7e-06), STAD (P=0.0013), COAD (P=2.3e-12), BRCA (P=0.012), SARC (P=2.8e-07), LIHC (P=0.01), UCEC (P=4.3e-0.5), PRAD (P=6.3e-06) and LUAD (P=0.0098). Subsequently, the association between CDC45 expression and neoantigens in different cancers was explored, and the data (Fig. 5C) illustrated that CDC45 expression was positively associated with neoantigens in LUAD (P=0.0045), BRCA (P=3.5e-13), UCEC (P=0.00023), STAD (P=0.0011), BLCA (P=0.011), and PRAD (P=9.1e-05). In addition, the association between CDC45 expression and Estimation of stromal and immune cells in malignant tumor tissues using expression data (ESTIMATE) and checkpoints was analyzed (Fig. S3). Moreover, the different immune subtypes were also analyzed across various cancers using TISIDB, including C1 (wound healing), C2 (IFN-γ dominant), C3 (inflammatory), C4 (lymphocyte depleted), C5 (immunologically quiet) and C6 (TGF-β dominant). A significant difference in CDC45 expression was observed in ACC, BLCA, BRCA, COAD, ESCA, KIRC, KIRP, LGG, LIHC, LUAD, LUSC, MESO, OV, PAAD, PRAD, SARC, STAD, TGCT, THCA, UCEC, and UCS. Taking COAD as an example, the C2 subtype exhibited the highest CDC45 expression while the C6 subtype exhibited low CDC45 levels (Fig. 5D). These

results indicated that CDC45 expression is associated with the immunology of various tumors.

CDC45 and m⁶A in various cancers. To further explore the potential roles of CDC45, it was hypothesized that CDC45 levels are related to m^{6}A methylation, which is the most abundant modification in eukaryotic cells (19). According to the literature, the core genes of m^{6}A methylation, including m^{6}A methyltransferase 'writers' (CBLL1, KIAA1429, METTL14, METTL3, RBM15, RBM15B, and WTAP), 'readers' (HNRNPA2B1, HNRNPC, IGF2BP1, IGF2BP2, IGF2BP3, RBMX, YTHDC1, YTHDC2, YTHDF1, YTHDF2, YTHDF3, and ZNF217) and 'erasers' (ALKBL5 and FTO) (20-23) were summarized; hence, the correlation between CDC45 expression and those genes was analyzed. The results revealed that CDC45 expression was primarily positively correlated with 'writers' and 'readers' in various cancers but negatively correlated with the 'reader' in THYM (Fig. 6A and B). However, the correlation between CDC45 levels and 'eraser' varied across different cancers (Fig. 6C). The REPIC database was then searched, and the data showed that CDC45 may be regulated by m^{6}A posttranslational modification (Fig. S4). These results were further demonstrated using the m^{6}A-Atlas database, where a total of 9 studies elucidated the m^{6}A positions of CDC45 in different cell lines and tissues (HeLa, HepG2, 293T, 293, ESC, and HCT116) using different techniques (Fig. 6D). The distribution of all the m^{6}A sites of CDC45 located on chr 22 (GSE63753) (31) are as follows: 19468535, 19470283, 19484961, 19491689, 19492898, 19495817, 19496177, 19496202, 19502339, 19504159, 19508041, 19508071, respectively (Fig. 6E and F), and 27 RBPs were obtained, including HNRNPC, RBM15 and YTHDC1 (Fig. 6G), which may be immediately regulated through the m^{6}A site. These results indicated that CDC45 participates in tumorigenesis via m^{6}A posttranslational modification in tumorigenesis.

CDC45 and GO/KEGG analysis. To further explore the biological significance of CDC45 in tumorigenesis in various cancers, gene co-expression analysis was first performed, and the results showed that CDC45 was significantly correlated with various cancers (Fig. S5). Next, CDC45-binding proteins were screened using the STRING database. Their interaction networks are shown in Fig. 7A, and a total of 50 interactive genes validated by experimental studies were obtained for further research. Another database, GEPIA2, was searched, and the top 100 genes co-expressed with CDC45 were obtained. Subsequently, the data of those genes was combined to perform the GO and KEGG analysis, and the identified biological process (BP) was linked to 'DNA replication', 'cell cycle G1/S phase transition', 'G1/S transition of mitotic cell cycle', 'DNA-dependent DNA replication' and 'DNA replication initiation' (Fig. 7B), while the cellular component (CC) showed that those genes were primarily enriched in 'chromosomal region', 'chromosome telomeric region', 'replication fork', 'nuclear replication fork' and 'MCM complex' (Fig. 7C). Finally, the molecular function (MF) of those genes included 'catalytic activity acting on DNA', 'DNA replication origin binding', 'single-strand DNA binding', 'DNA helicase activity' and '3'-5' DNA helicase activity' (Fig. 7D). The KEGG pathway analysis indicated
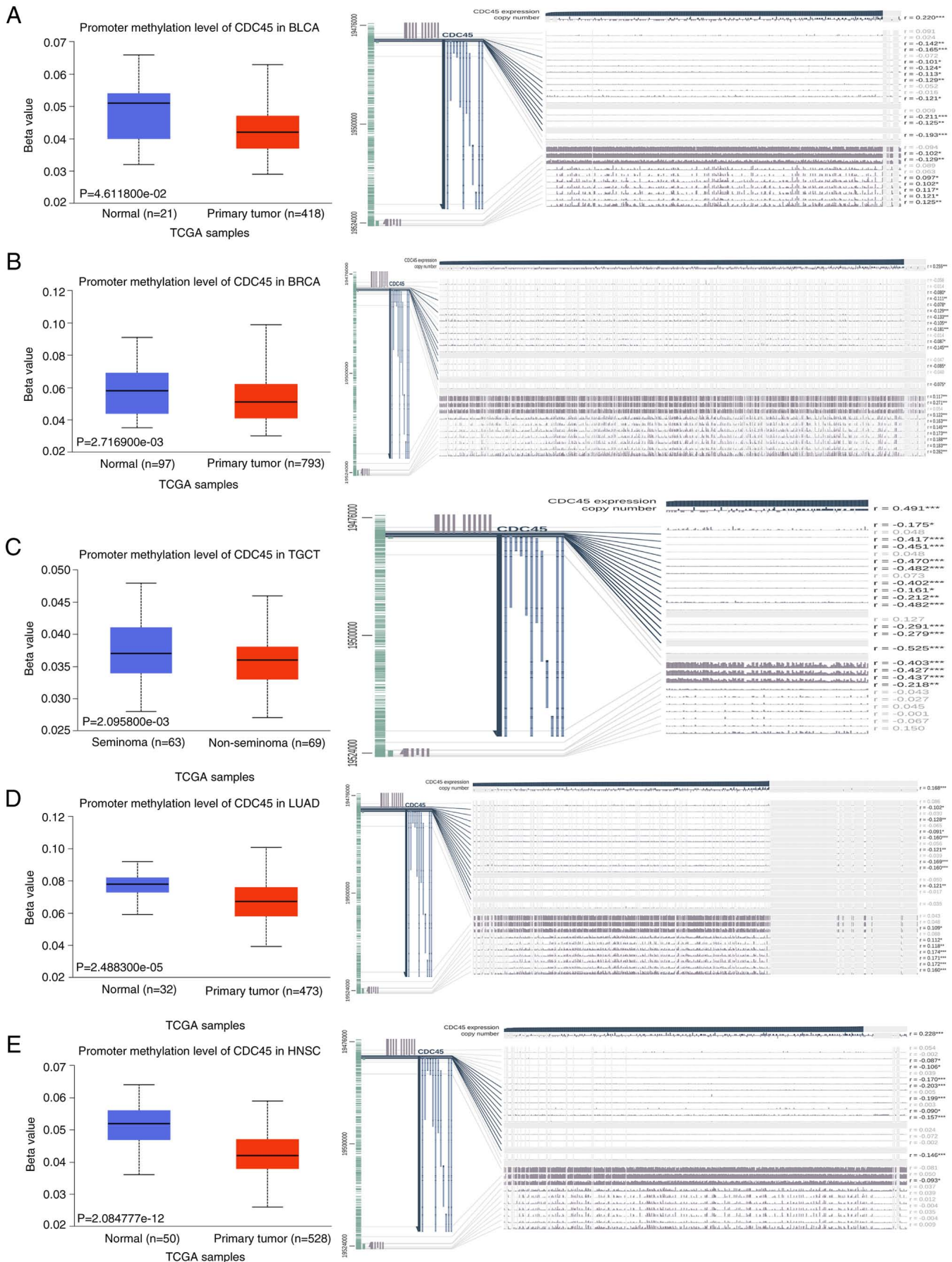
Figure 4. DNA promoter methylation levels of CDC45 between tumors and matched control tissues were determined using UALCAN (left) and details (right) in (A) BLCA, (B) BRCA, (C) TGCT, (D) LUAD and (E) HNSC. *P<0.05, **P<0.01 and ***P<0.001. CDC45, cell division cycle 45; BLCA, bladder urothelial carcinoma; BRCA, breast invasive carcinoma; TGCT, testicular germ cell tumors; LUAD, lung adenocarcinoma; HNSC, head and neck squamous cell carcinoma.
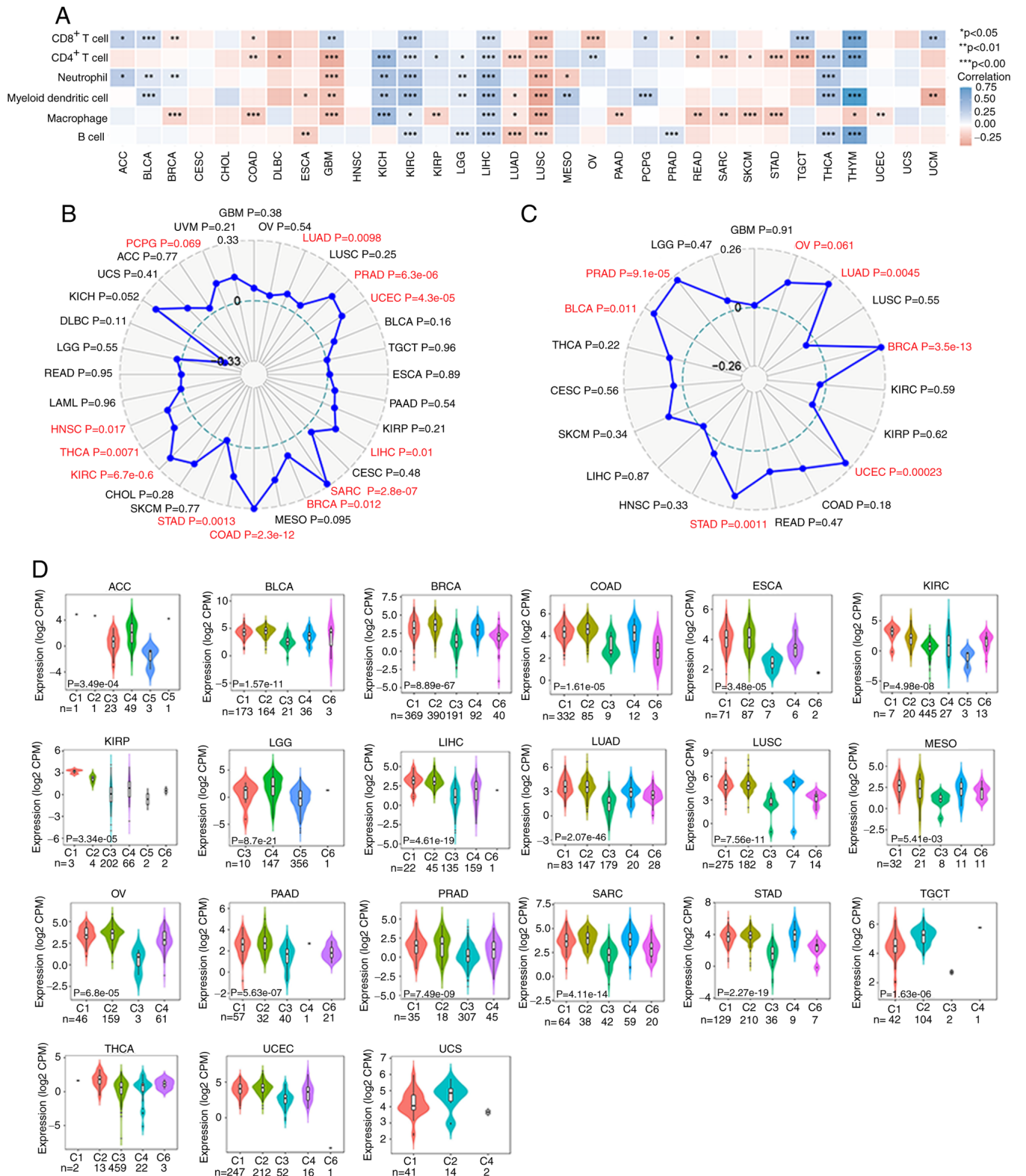
Figure 5. Association between CDC45 expression and immunity in various cancers. (A) The association between CDC45 and CD8+ T cells, CD4+ T cells, neutrophils, myeloid dendritic cells, macrophages, and B cells across all TCGA cancers in the TIMER2.0 database. (B) The association between CDC45 and MSI and between CDC45 and neoantigens (C) in various cancers. (D) The association between CDC45 and different immune subtypes across various cancers via TISIDB. *P<0.05, **P<0.01 and ***P<0.001. CDC45, cell division cycle 45; TCGA, The Cancer Genome Atlas; TIMER, Tumor Immune Estimation Resource; TISIDB, tumor-immune system interactions database; MSI, microsatellite instability GBM, glioblastoma; OV, ovarian serous cystadenocarcinoma; LUAD, lung adenocarcinoma; LUSC, lung squamous cell carcinoma; PRAD, prostate adenocarcinoma; UCEC, uterine corpus endometrial carcinoma; BLCA, bladder urothelial carcinoma; TGCT, testicular germ cell tumors; ESCA, esophageal carcinoma; PAAD, pancreatic adenocarcinoma; KIRP, kidney renal papillary cell carcinoma; LIHC, liver hepatocellular carcinoma; CESC, cervical squamous cell carcinoma and endocervical adenocarcinoma; SARC, sarcoma; BRCA, breast invasive carcinoma; MESO, mesothelioma; COAD, colon adenocarcinoma; STAD, stomach adenocarcinoma; SKCM, skin cutaneous melanoma; CHOL, cholangiocarcinoma; KIRC, kidney renal clear cell carcinoma; THCA, thyroid carcinoma; HNSC, head and neck squamous cell carcinoma; LAML, acute myeloid leukemia; READ, rectum adenocarcinoma; LGG, brain lower grade glioma; DLBC, diffuse large B-cell lymphoma; KICH, kidney chromophobe; UCS, uterine carcinosarcoma; ACC, adrenocortical carcinoma; PCPG, pheochromocytoma and paraganglioma; UVM, uveal melanoma.
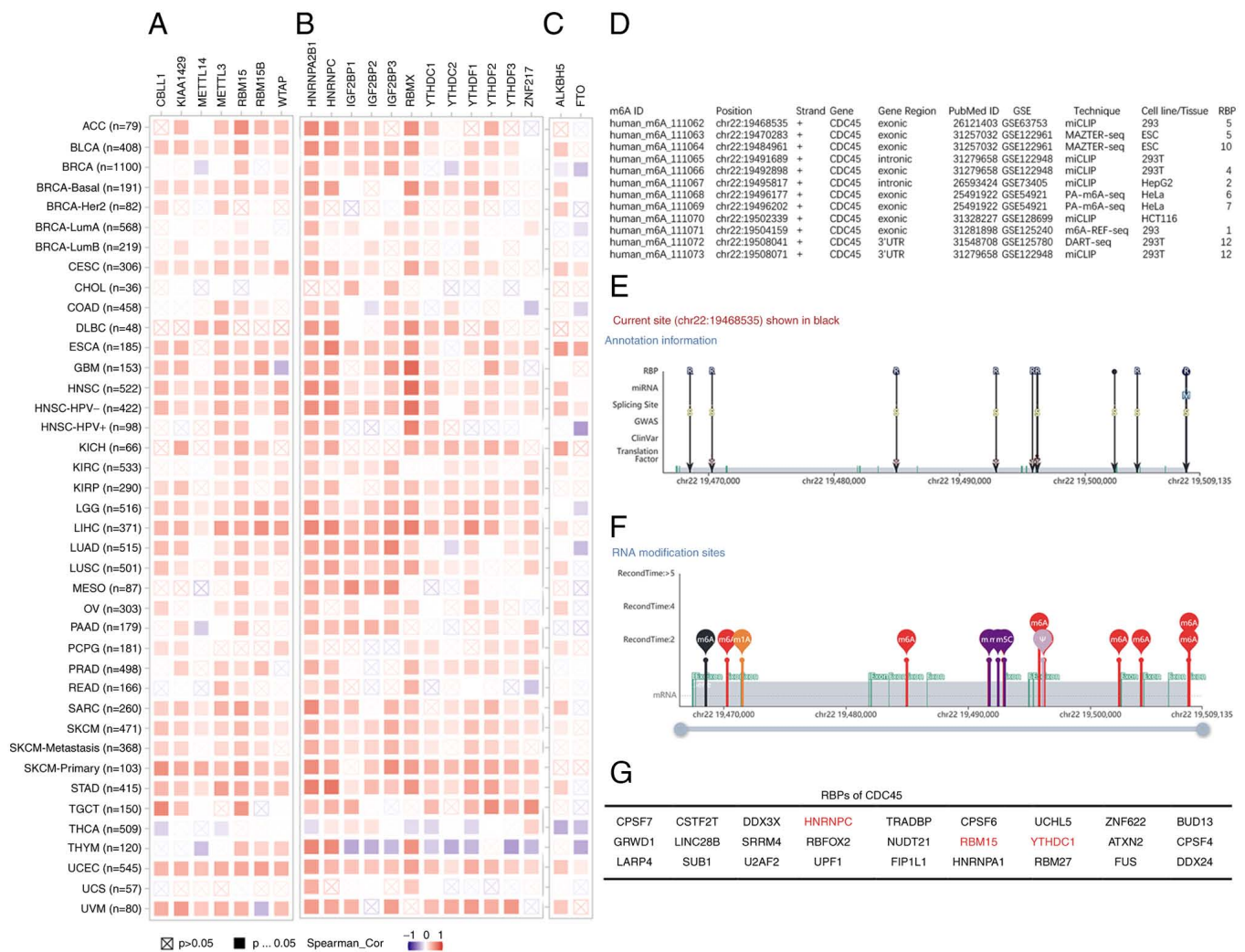
Figure 6. CDC45 expression and m⁶A in various cancers. The correlation between CDC45 expression and m⁶A (A) 'writers', (B) 'readers' and (C) 'erasers' was determined using TIMER 2.0. (D) Summary of CDC45 and m⁶A posttranslational modification by m⁶A-Atlas. (E and F) The landscape of all the m⁶A sites and RNA modification sites of CDC45 from GSE63753. (G) The RBPs of CDC45 collected from m⁶A-Atlas. CDC45, cell division cycle 45; m⁶A, N^6-methyladenosine; RBPs, RNA binding proteins; ACC, adrenocortical carcinoma; BLCA, bladder urothelial carcinoma; BRCA, breast invasive carcinoma; CESC, cervical squamous cell carcinoma and endocervical adenocarcinoma; CHOL, cholangiocarcinoma; COAD, colon adenocarcinoma; DLBC, diffuse large B-cell lymphoma; ESCA, esophageal carcinoma; GBM, glioblastoma; HNSC, head and neck squamous cell carcinoma; KICH, kidney chromophobe; KIRC, kidney renal clear cell carcinoma; KIRP, kidney renal papillary cell carcinoma; LGG, brain lower grade glioma; LIHC, liver hepatocellular carcinoma; LUAD, lung adenocarcinoma; LUSC, lung squamous cell carcinoma; MESO, mesothelioma; OV, ovarian serous cystadenocarcinoma; PAAD, pancreatic adenocarcinoma; PCPG, pheochromocytoma and paraganglioma; PRAD, prostate adenocarcinoma; READ, rectum adenocarcinoma; SARC, sarcoma; SKCM, skin cutaneous melanoma; STAD, stomach adenocarcinoma; TGCT, testicular germ cell tumors; THCA, thyroid carcinoma; THYM, thymoma; UCEC, uterine corpus endometrial carcinoma; UCS, uterine carcinosarcoma; UVM, uveal melanoma.

that CDC45 was involved in the 'cell cycle', 'DNA replication', 'nucleotide excision repair', 'Fanconi anemia pathway' and 'mismatch repair' in the tumorigenesis of various cancers (Fig. 7E). These results were further supported by three other databases BioGRID, HIPPIE and HitPredict (Fig. S6).

Biological functions of CDC45 in vitro. Considering the biases of bioinformatics analysis, *in vitro* experiments were next performed to validate the biological functions of CDC45. Following transfection with siRNA, CDC45 expression in U87 and U251 cells was assessed by RT-qPCR (Fig. 8A). CCK-8 assays were then performed, and the results revealed that knockdown of CDC45 inhibited the proliferation of U87 and U251 cells (Fig. 8B). These results were further

supported by the EdU proliferation assay, which revealed that EdU-positive cells were higher in the control group than in the CDC45-knockdown group (Fig. 8C). Finally, cell cycle analysis was also conducted. After knocking down CDC45, cell cycle progression was primarily arrested at the G1 phase (Fig. 8D). These results revealed that CDC45 represents an oncogene in GBM.

Discussion

CDC45, which is composed of 650 amino acids, was first identified as having a key role in chromosomal DNA replication in budding yeast (24). Thereafter, accumulating studies have explored the functions of CDC45 in various conditions, and it has been demonstrated that CDC45 is part of the helicase
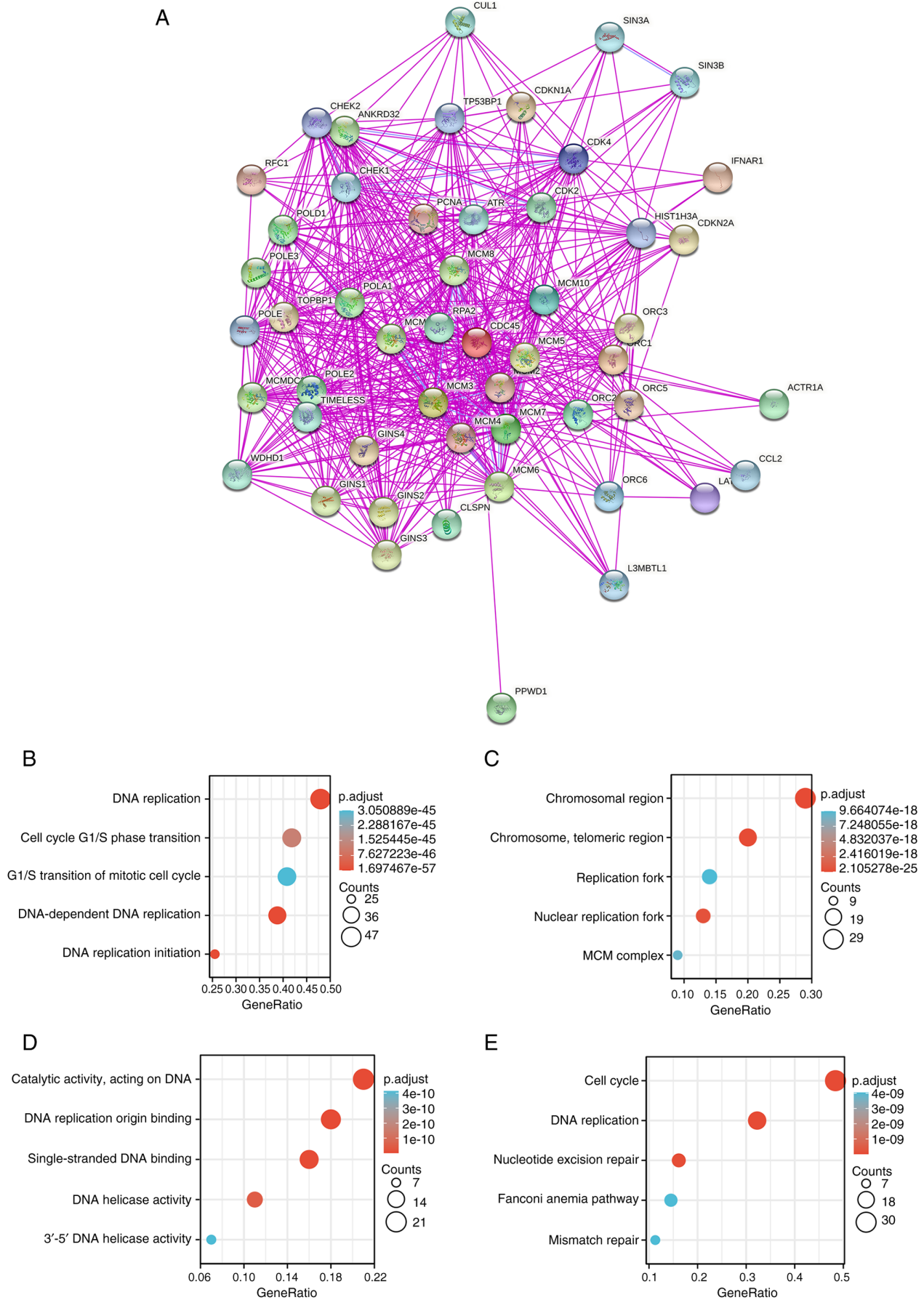
Figure 7. Functional enrichment analysis of CDC45 in various cancers. (A) The PPI network of CDC45 according to STRING. GO enrichment analysis of (B) BP, (C) CC and (D) MF. (E) KEGG enrichment analysis of CDC45-binding proteins. CDC45, cell division cycle 45; PPI, protein-protein interaction; STRING, Search Tool for the Retrieval of Interacting Genes/Proteins; GO, Gene Ontology; BP, biological process; CC, cellular component; MF, molecular function; KEGG, Kyoto Encyclopedia of Genes and Genomes.
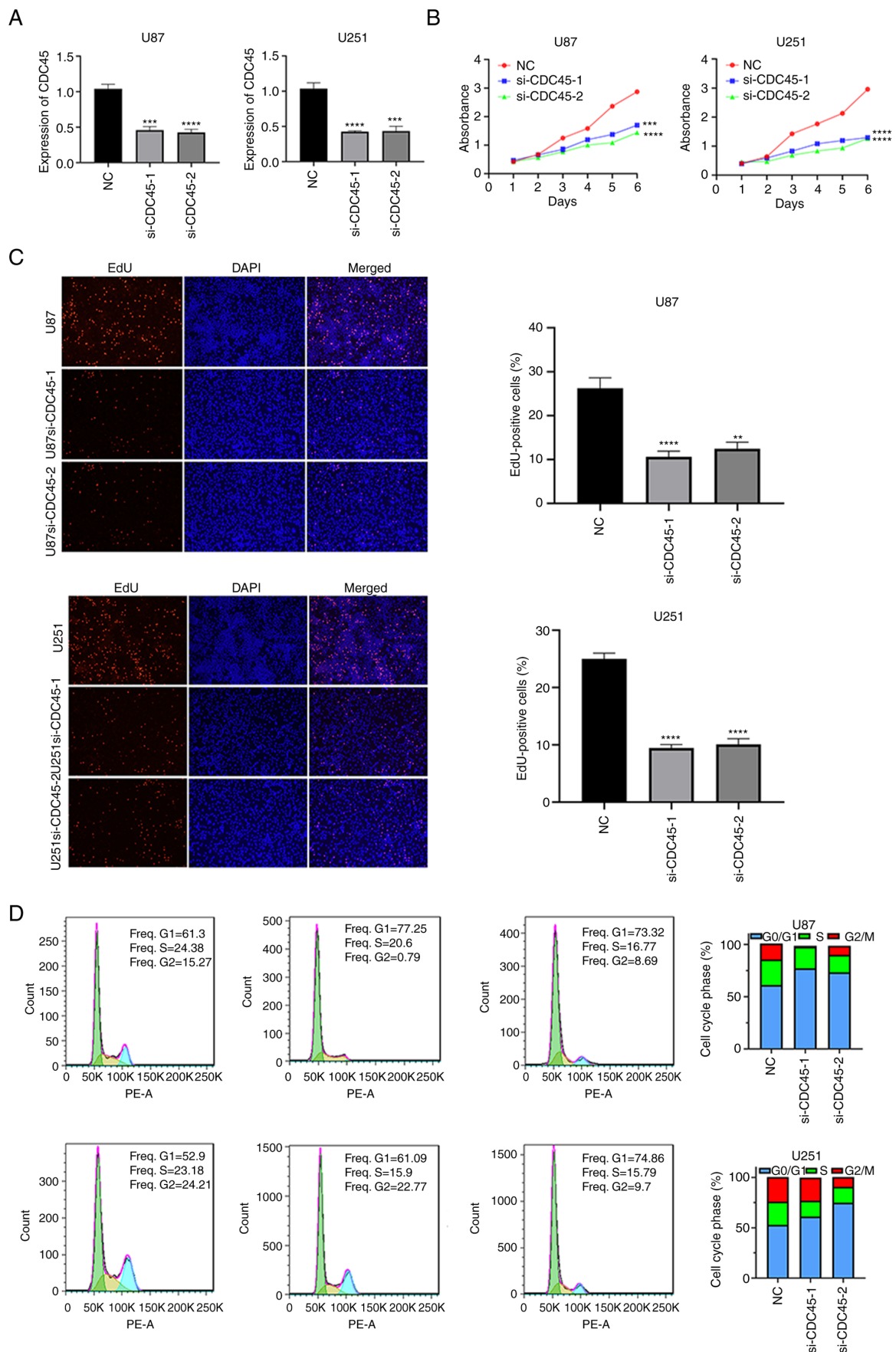
Figure 8. Biological functions of CDC45 *in vitro*. (A) CDC45 mRNA expression was detected by PCR after transfection with siRNA in U87 and U251 cells. (B) CCK-8 assays were performed after transfection with CDC45 siRNA in U87 and U251 cells. (C) EdU assays were used to detect the proliferative ability of U87 and U251 cells. Scale bar, 10 μm. (D) Flow cytometry was adopted to determine cell cycle changes in response to CDC45 knockdown in U87 and U251 cells. CDC45, cell division cycle 45; siRNA, small interfering RNA; CCK-8, Cell Counting Kit-8; EdU, 5-ethynyl-2'-deoxyuridine; NC, negative control. **$P<0.01$, ***$P<0.001$, ****$P<0.0001$.

complex (CDC45-MCM2-7/GINS), which regulates the initiation of DNA replication (25-27). Although several studies have demonstrated that CDC45 serves as an oncogene (9,15,18), whether CDC45 can play a role in the pathogenesis of different tumors through certain common molecular mechanisms remains to be answered. Through a literature search, no publication was retrieved with a pan-cancer analysis of CDC45 from the perspective of overall tumors. Thus, the CDC45 gene was comprehensively examined in a total of 33 different tumors based on the data of different databases and the molecular features of gene expression, genetic alteration, DNA methylation, immunology, or GO/KEGG analysis. Thus, the comprehensive analysis of CDC45 in various cancers was conducted.

In the present study, CDC45 expression was first analyzed between various cancers and their matched control tissues, and the data revealed that CDC45 expression was highly expressed in most cancers. Moreover, overexpressed CDC45 levels conveyed poor OS and DFS prognosis in 13 cancer types, while CESC and OV exhibited the opposite trend, indicating that CDC45 may be an oncogene. Unfortunately, only one experimental study has been performed focusing on THCA, however the result of this study was consistent with our finding (18). Fundamental studies in other cancers are still required.

Given that gene mutations may participate in numerous processes of tumorigenesis (1,28), it was then explored whether mutations of CDC45 participated in the development of cancers. The cBioPortal database, which contains TCGA data, was used to analyze the CDC45 mutations, and the results showed that the most frequent genetic alteration was the 'amplification' type, followed by 'mutation', 'deep deletion' and 'structure variant' types. Unfortunately, the original data for the survival analyses was not retrieved, and thus, the absence of such data is a limitation of the present study.

DNA promoter methylation participates in a number of biological processes. Numerous studies have demonstrated the mechanisms of DNA methylation and histone modification among different cancers, especially the CpG island promoter hypermethylation of tumor suppressor genes (29,32,33). Therefore, methylation in CDC45 promoter regions was explored in the present study. The UALCAN database was adopted and identified five types of cancers that exhibited low methylation levels compared with matched normal samples, including BLCA, BRCA, TGCT, LUAD and HNSC (all P<0.05), indicating that the low methylation levels in those cancers lead to CDC45 overexpression. Another database, MEXPRESS (26), was also searched to verify this result, and the data confirmed low methylation levels in those cancers. These results indicated that CDC45 methylation may participate in the processes of tumorigenesis.

Due to the important roles of immunotherapy in the treatment of cancers (34,35), potential correlations between CDC45 levels and different immune cells across various cancers were investigated. The MSI, neoantigen and immune subtypes were also explored in different cancers. CDC45 was positively correlated with the immune cells in KIRC, LIHC, THCA and THYM but negatively correlated with those in LUAD, LUSC, and GBM. However, none of these

studies (8-18) focused on CDC45 expression or immunology across different cancers. The findings of the present study, are the first to the best of our knowledge, to suggest correlations between CDC45 expression and tumor immunity in certain cancers.

Accumulating evidence has illustrated the functions and roles of m6A methylation in different cancers. There are three types of enzymes known as 'readers', 'writers' and 'erasers' (20-22,36). These genes were collected and a correlation analysis between CDC45 expression and these genes was performed. The data revealed that CDC45 was primarily positively correlated with 'writers' and 'erasers', and these results were further supported by data from the m6A-Atlas database (21,31,37). All RBPs in different GSE data were also downloaded and it was determined that HNRNPC, RBM15 and YTHDC1 may be directly regulated through m6A sites. Data from the REPIC database was consistent with these results, and additional experimental evidence is required for the potential association between CDC45 and m6A in various cancers.

Subsequently, GO and KEGG analyses were performed. GO contains three categories: CC, MF and BP, which can aid in better understanding the functions of these genes (38). The results revealed that CDC45 may have a potential impact on 'chromosomal region', 'DNA replication', 'catalytic activity, acting on DNA' and 'cell cycle' pathways, and the cell cycle analysis revealed that these results were consistent with previous studies (39,40).

Finally, the association between CDC45 expression and the predictive ability of OS in different cancers was assessed. The results demonstrated that CDC45 expression was negatively associated with the survival probability in ACC, KICH, KIRC, KIRP, LGG, LIHC, LUAD, MESO, PAAD, PCPG, SARC, READ, and UCEC (all P<0.05) but positively associated with DLBC (P=0.011). The ROC curve of CDC45 expression showed a high predictive value for ACC, MESO, KICH and KIRP. These results indicated that CDC45 expression may be a biomarker for the prognosis of those cancers, and additional clinical studies are required to clarify these potential predictive values in different cancers. This research, however, is subject to several limitations. First, the present study focused on the possible mechanisms of CDC45 in 33 cancers, and the specific mechanism of CDC45 for certain cancers was not explored. Second, *in vivo* experiments were not performed to investigate the biological functions of CDC45. Therefore, further fundamental studies are still required to verify the mechanisms of CDC45. Finally, as single-cell analysis aids in better understanding and characterizing cell types and their functions regarding pathophysiological processes based on molecular signatures, it has emerged as a powerful tool for resolving intratumor heterogeneity, delineating stromal cell types, and detecting rare subpopulations (Fig. S7).

In summary, CDC45 expression and survival analysis was first explored in multiple cancer types. The potential mechanisms of CDC45 were then explored, including gene alterations, DNA promoter methylation, different immune cells, m6A, GO and KEGG enrichment analysis. The potential predictive values of CDC45 in different cancers were also identified. The results revealed that CDC45 is an oncogene and provide a potential target in multiple cancers.

Acknowledgements

Availability of data and materials

The data that support the present findings of this study are available from TCGA and GTEx online databases.

Authors' contributions

YL, XC and FL performed the experiments and compiled the manuscript. HY and YZ contributed to the design of the study and analyzed data. KD and YN conducted the experiments and analyzed the data. QH contributed to the conception and design of the present study and revised the manuscript. YL and XC confirm the authenticity of all the raw data. All authors read and approved the final manuscript.

Ethics approval and consent to participate

Not applicable.

Patient consent for publication

Not applicable.

Competing interests

The authors declare that they have no competing interests.

References

1. Hanahan D and Weinberg RA: Hallmarks of cancer: The next generation. Cell 144: 646-674, 2011.
2. Boshuizen J and Peeper DS: Rational cancer treatment combinations: An urgent clinical need. Mol Cell 78: 1002-1018, 2020.
3. Mun EJ, Babiker HM, Weinberg U, Kirson ED and Von Hoff DD: Tumor-treating fields: A fourth modality in cancer treatment. Clin Cancer Res 24: 266-275, 2018.
4. Ilves I, Petojevic T, Pesavento JJ and Botchan MR: Activation of the MCM2-7 helicase by association with Cdc45 and GINS proteins. Mol Cell 37: 247-258 2010.
5. Boos D, Frigola J and Diffley JF: Activation of the replicative DNA helicase: Breaking up is hard to do. Curr Opin Cell Biol 24: 423-430, 2012.
6. Tanaka S and Araki H: Helicase activation and establishment of replication forks at chromosomal origins of replication. Cold Spring Harb Perspect Biol 5: a010371, 2013.
7. Owens JC, Detweiler CS and Li JJ: CDC45 is required in conjunction with CDC7/DBF4 to trigger the initiation of DNA replication. Proc Natl Acad Sci USA 94: 12521-12526, 1997.
8. Feng D, Tu Z, Wu W and Liang C: Inhibiting the expression of DNA replication-initiation proteins induces apoptosis in human cancer cells. Cancer Res 63: 7356-7364, 2003.
9. Pollok S, Bauerschmidt C, Sänger J, Nasheuer HP and Grosse F: Human Cdc45 is a proliferation-associated antigen. FEBS J 274: 3669-3684, 2007.
10. Srinivasan SV, Dominguez-Sola D, Wang LC, Hyrien O and Gautier J: Cdc45 is a critical effector of myc-dependent DNA replication stress. Cell Rep 3: 1629-1639, 2013.
11. Hu Y, Wang L, Li Z, Wan Z, Shao M, Wu S and Wang G: Potential prognostic and diagnostic values of CDC6, CDC45, ORC6 and SNHG7 in colorectal cancer. Onco Targets Ther 12: 11609-11621, 2019.
12. Huang J, Li Y, Lu Z, Che Y, Sun S, Mao S, Lei Y, Zang R, Li N, Zheng S, et al: Analysis of functional hub genes identifies CDC45 as an oncogene in non-small cell lung cancer-a short report. Cell Oncol (Dordr) 42: 571-578, 2019.
13. Piao J, Sun J, Yang Y, Jin T, Chen L and Lin Z: Target gene screening and evaluation of prognostic values in non-small cell lung cancers by bioinformatics analysis. Gene 647: 306-311, 2018.
14. Ke Y, Guo W, Huang S, Li Y, Guo Y, Liu X, Jin Y and Ma H: RYBP inhibits esophageal squamous cell carcinoma proliferation through downregulating CDC6 and CDC45 in G1-S phase transition process. Life Sci 250: 117578, 2020.
15. Lu HP, Du XF, Li JD, Huang SN, He RQ, Wu HY, Li MF, Wu WZ, Chen JT, Mo WJ and Chen G: Expression of cell division cycle protein 45 in tissue microarrays and the CDC45 gene by bioinformatics analysis in human hepatocellular carcinoma and patient outcomes. Med Sci Monit 27: e928800, 2021.
16. Sang L, Wang XM, Xu DY and Zhao WJ: Bioinformatics analysis of aberrantly methylated-differentially expressed genes and pathways in hepatocellular carcinoma. World J Gastroenterol 24: 2605-2616, 2018.
17. Xiang XH, Yang L, Zhang X, Ma XH, Miao RC, Gu JX, Fu YN, Yao Q, Zhang JY, Liu C, et al: Seven-senescence-associated gene signature predicts overall survival for asian patients with hepatocellular carcinoma. World J Gastroenterol 25: 1715-1728, 2019.
18. Sun J, Shi R, Zhao S, Li X, Lu S, Bu H and Ma X: Cell division cycle 45 promotes papillary thyroid cancer progression via regulating cell cycle. Tumour Biol 39: 1010428317705342, 2017.
19. Deng M, Brägelmann J, Schultze JL and Perner S: Web-TCGA: An online platform for integrated analysis of molecular cancer data sets. BMC Bioinformatics 17: 72, 2016.
20. Ru B, Wong CN, Tong Y, Zhong JY, Zhong SS, Wu WC, Chu KC, Wong CY, Lau CY, Chen I, et al: TISIDB: An integrated repository portal for tumor-immune system interactions. Bioinformatics 35: 4200-4202, 2019.
21. Li T, Fu J, Zeng Z, Cohen D, Li J, Chen Q, Li B and Liu XS: TIMER2.0 for analysis of tumor-infiltrating immune cells. Nucleic Acids Res 48: W509-W514, 2020.
22. Thul PJ and Lindskog C: The human protein atlas: A spatial map of the human proteome. Protein Sci 27: 233-244, 2018.
23. Cerami E, Gao J, Dogrusoz U, Gross BE, Sumer SO, Aksoy BA, Jacobsen A, Byrne CJ, Heuer ML, Larsson E, et al: The cBio cancer genomics portal: An open platform for exploring multidimensional cancer genomics data. Cancer Discov 2: 401-404, 2012.
24. Tang Z, Kang B, Li C, Chen T and Zhang Z: GEPIA2: An enhanced web server for large-scale expression profiling and interactive analysis. Nucleic Acids Res 47: W556-W560, 2019.
25. Chandrashekar DS, Bashel B, Balasubramanya SA, Creighton CJ, Ponce-Rodriguez I, Chakravarthi BV and Varambally S: UALCAN: A portal for facilitating tumor subgroup gene expression and survival analyses. Neoplasia 19: 649-658, 2017.
26. Koch A, Jeschke J, Van Criekinge W, van Engeland M and De Meyer T: MEXPRESS update 2019. Nucleic Acids Res 47: W561-W565, 2019.
27. Tang Y, Chen K, Song B, Ma J, Wu X, Xu Q, Wei Z, Su J, Liu G, Rong R, et al: m6A-Atlas: A comprehensive knowledgebase for unraveling the N6-methyladenosine (m6A) epitranscriptome. Nucleic Acids Res 49: D134-D143, 2021.
28. Liu S, Zhu A, He C and Chen M: REPIC: A database for exploring the N6-methyladenosine methylome. Genome Biol 21: 100, 2020.
29. von Mering C, Huynen M, Jaeggi D, Schmidt S, Bork P and Snel B: STRING: A database of predicted functional associations between proteins. Nucleic Acids Res 31: 258-261, 2003.
30. Livak KJ and Schmittgen TD: Analysis of relative gene expression data using real-time quantitative PCR and the 2(-Delta Delta C(T)) method. Methods 25: 402-408, 2001.
31. Linder B, Grozhik AV, Olarerin-George AO, Meydan C, Mason CE and Jaffrey SR: Single-nucleotide-resolution mapping of m6A and m6Am throughout the transcriptome. Nat Methods 12: 767-772, 2015.

32. Herman JG and Baylin SB: Gene silencing in cancer in association with promoter hypermethylation. N Eng J Med 349: 2042-2054, 2003.
33. Esteller M: Aberrant DNA methylation as a cancer-inducing mechanism. Annu Rev Pharmacol Toxicol 45: 629-656, 2005.
34. Fesnak AD, June CH and Levine BL: Engineered T cells: The promise and challenges of cancer immunotherapy. Nat Rev Cancer 16: 566-581, 2016.
35. Hu Z, Ott PA and Wu CJ: Towards personalized, tumour-specific, therapeutic vaccines for cancer. Nat Rev Immunol 18: 168-182, 2018.
36. He L, Li H, Wu A, Peng Y, Shu G and Yin G: Functions of N6-methyladenosine and its role in cancer. Mol Cancer 18: 176, 2019.
37. Garcia-Campos MA, Edelheit S, Toth U, Safra M, Shachar R, Viukov S, Winkler R, Nir R, Lasman L, Brandis A, *et al*: Deciphering the 'm6A Code' via antibody-independent quantitative profiling. Cell 178: 731-747.e16, 2019.
38. Gene Ontology Consortium: Gene ontology consortium: Going forward. Nucleic Acids Res 43: D1049-D1056, 2015.
39. Broderick R and Nasheuer HP: Regulation of Cdc45 in the cell cycle and after DNA damage. Biochem Soc Trans 37: 926-930, 2009.
40. Köhler C, Koalick D, Fabricius A, Parplys AC, Borgmann K, Pospiech H and Grosse F: Cdc45 is limiting for replication initiation in humans. Cell Cycle 15: 974-985, 2016.